Dalton Transactions

ROYAL SOCIETY OF CHEMISTRY

COMMUNICATION

View Article Online
View Journal | View Issue

Cite this: *Dalton Trans.*, 2025, **54**, 12754

Received 17th April 2025,
Accepted 5th June 2025

DOI: 10.1039/d5dt00918a

rsc.li/dalton

Hydrogen bonds in the second coordination sphere of metal complexes in the gas phase – playing by the rules?†

Dušan P. Malenov, *[a] Jelena M. Živković[b] and Snežana D. Zarić *[a]

Hydrogen bonds in the second coordination sphere of metal complexes play a crucial role in the fine-tuning of their chemical and physical properties, including catalytic activity and selectivity. Our gas-phase computational study on hydrogen bonds of 180 aqua and ammine complexes of transition metals indicates that hydrogen bond energy depends on the charge of the complex, as well as on the ratio between the metal oxidation state (OS) and metal coordination number (CN), and is independent of the geometry of the complex, metal type and nature of other ligands. We have determined a linear increase in interaction energy with the increase in charge, as well as a linear increase of interaction energy with the increase in the OS/CN value. Based on the data presented in this work, we can predict and tune energies of hydrogen bonds in the second coordination sphere of metal complexes. That is, ligands of the same type in complexes with the same charge and the same OS/CN ratio will form hydrogen bonds with very similar energies, independent of all other factors.

Noncovalent interactions in the second coordination sphere of metal complexes, as well as the composition of the metal complex, have been recognized as important factors in the fine-tuning of the chemical and physical properties of such systems. Because of that, these interactions have been used in numerous areas such as molecular recognition, synthesis, materials, separation of metals, medicine, catalysis, biochemistry and environmental science.[1–4]

Coordination of molecules to transition metal atoms influences the properties of coordinated molecules.[5–22] It was observed that coordination can cause bond weakening in ligands and influences pK_a values.[13–18] Extensive studies on coordinated water, ammonia, ethylenediamine and amino acids to metals have shown the influence of coordination on hydrogen bonds.[5–9,21–23] Data from the crystal structures and quantum chemical calculations have shown that coordination makes hydrogen bonds of water, ammonia, and ethylenediamine stronger.[5–7,10,11]

Hydrogen bonds can be important in catalytic processes, including the ones involving transition metal complexes, such as hydroformylation, hydrogenation, C–H activation, radical-type transformations, and oxidation.[12,24–36] It is important that noncovalent interactions have a weak and reversible nature that enables the restoration of the second coordination spheres after a catalytic cycle. It has been discovered recently that hydrogen bonds in the second coordination sphere of metal complexes can be used to control the activity and selectivity of catalysts. This can be improved by hydrogen bonds between coordinated ligands or between ligands and substrates, which help to pre-organize substrates.[24] By using this strategy, significantly better selectivity can be obtained than that by using a traditional catalyst.[24]

In this work we present data on hydrogen bonds of coordinated water and ammonia in 180 metal complexes. These data enable us to study the influence of various factors on the strength of hydrogen bonds: charge of the complex, metal oxidation state (OS), metal coordination number (CN), metal atomic number (considering different metals of the same transition row as well as metals from different transition rows), as well as the nature of other ligands.

The calculations of hydrogen bonds of water and ammonia coordinated to a metal with an uncoordinated (free) water molecule (Fig. 1) were performed in the gas phase using the Gaussian 09 (version D.01) program package.[37] The hydrogen bonds of metal complexes with charges from 0 to 3+ were calculated using the M06 method[38] with D3 dispersion correction[39] and def2-TZVPP basis set.[40] This level of theory was shown in our previous work to be in good agreement with the CCSD(T)/CBS level for hydrogen bonds of ammine complexes (Table S1†).[6] Further details on calculations are given in the ESI.†

[a]*University of Belgrade – Faculty of Chemistry, Studentski trg 12-16, 11000 Belgrade, Serbia. E-mail: malenov@chem.bg.ac.rs, szaric@chem.bg.ac.rs*
[b]*Innovative Centre of the Faculty of Chemistry, Studentski trg 12–16, 11000 Belgrade, Serbia*

†Electronic supplementary information (ESI) available: Computational details, details on interaction energies and their components, cartesian coordinates for all studied systems. See DOI: https://doi.org/10.1039/d5dt00918a

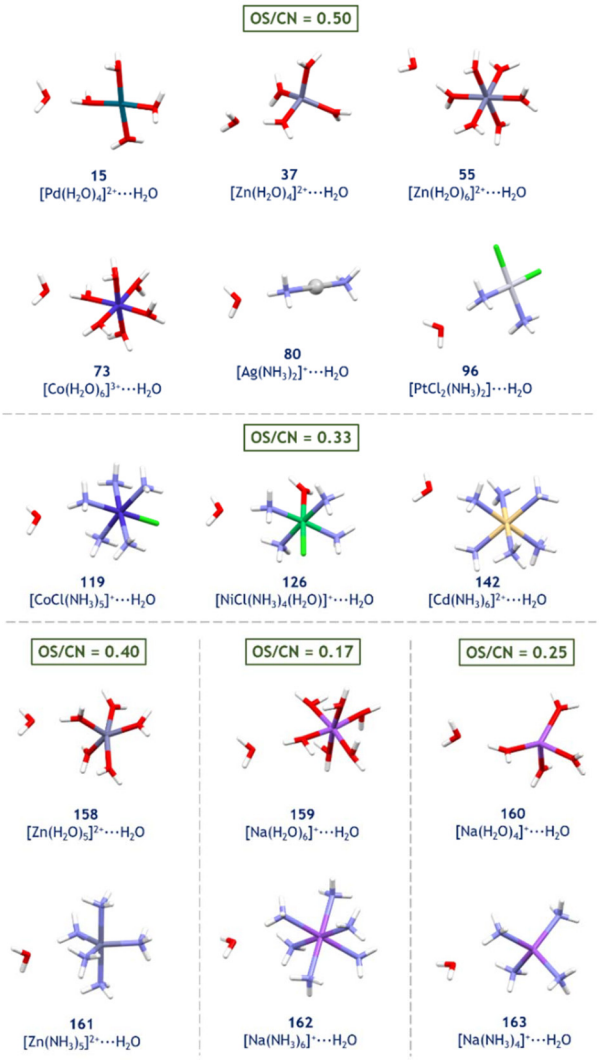

Fig. 1 Examples of hydrogen bonds formed between free water and aqua and ammine complexes studied in this work.

Our primary data set contains hydrogen bonds between coordinated water (systems **3–78**) and ammonia (systems **79–157**, ESI†) as hydrogen bond donors and free water as a hydrogen bond acceptor. Coordinated water and ammonia are ligands in linear, square planar, tetrahedral and octahedral complexes, with metals in various oxidation states. To study the hydrogen bonds of complexes with different charges, chloride ligands were incorporated (Fig. 1, Table 1 and Tables S2, S3, ESI†). Hydrogen bonds of several complexes with different coordination numbers and/or metal oxidation states were also included (systems **158–163**). Additionally, to gain further insight into the influence of ligands on hydrogen bonds, chloride ligands (π-donors) were replaced with cyanides (π-acceptors) (systems **164–182**). The examples of the hydrogen bonded structures are shown in Fig. 1, while the full list is given in the ESI.†

Electrostatic potential (ESP) is a very useful tool in studies on noncovalent interactions,[41] both qualitatively and quantitatively. Our previous data show linear correlation between hydrogen bond energies and the values of ESPs calculated on the interacting hydrogen atom of a coordinated ligand.[6–9,42] Our previous data also indicate important influence of the charge of the complexes on the strength of hydrogen bonds, as well as the influence of the oxidation state and coordination number.[6,7,9] As one can anticipate, the increase in the positive charge of the complex increases the strength of the hydrogen bonds of coordinated water and ammonia, since these ligands act as hydrogen bond donors (Fig. 1). Also, an increase of the oxidation state of the metal atom strengthens the hydrogen bonds, since the electrostatic potential on the interacting hydrogen atom increases.[6,7,9] The increase of the coordination number decreases the strength of hydrogen bonds, since the positive charge of the metal ion is distributed to a larger number of ligands.[6,7,9]

Data in this work, obtained from a significantly larger number of studied complexes, support these findings and provide general rules on hydrogen bonds of metal complexes. The data in Fig. 2 and Table 1 (also Tables S2 and S3 in the ESI†) show that the charge of the complex has the most important influence on the interaction energies. Considering the interaction energies one can notice the grouping of the complexes with different charges (Fig. 2). The energies of the hydrogen bonds of coordinated water are roughly between −8 and −10 kcal mol^{-1} for neutral complexes, between −11 and −16 kcal mol^{-1} for 1+ charged complexes, between −17 and −25 kcal mol^{-1} for 2+ charged complexes, and between −31 and −35 kcal mol^{-1} for complexes with charge 3+. The energies of the hydrogen bonds of coordinated ammonia are weaker; however, we see similar clustering based on the charge of the complex (Fig. 2).

In addition, Fig. 2 and Table 1 indicate subgroups of complexes with charges 1+ and 2+. Closer inspection of these subgroups showed that two subgroups of complexes with charge 1+ differ in the ratio of the oxidation state (OS) and coordination number (CN), OS/CN, namely, complexes with stronger interactions have an OS/CN value of 0.50, while complexes with weaker interactions have an OS/CN value of 0.33 (Fig. 2 and Table 1). The same was observed for 2+ charged complexes.

These data show that the OS/CN value is a very important factor and the one making the decisive influence on energies of hydrogen bonds both in aqua and ammine complexes. Accordingly, complexes can be categorized into types, depending on their charges and OS/CN values (Table 1); the complexes of the same type will have hydrogen bonds with very similar energies, regardless of the other factors. This interesting observation shows that the increase of the oxidation state (OS) by 1 and the decrease of the coordination number (CN) by 2 give very similar interaction energies. Hence, the complexes of Ag(I) with two ligands have very similar interaction energies (*e.g.* system **4**, −15.01 kcal mol^{-1}) to complexes of M(II) metals with four ligands (*e.g.* system **34**, −15.26 kcal mol^{-1}), and as Co(III) complexes with six ligands (*e.g.* system **65**, −15.12 kcal mol^{-1}, Table 1). All these complexes have an OS/CN value of 0.50. All complexes with M(II) and six ligands

Table 1 Classification of aqua and ammine complexes according to their hydrogen bonds. Chg stands for the charge of the complex, OS stands for the metal oxidation state, and CN stands for the metal coordination number. Electrostatic potentials at interacting hydrogen atoms (ESP, kcal mol^{-1}) on the 0.001 a.u. electron density contour, as well as H···O distances (d, Å) and M06L-D3/def2-TZVPP interaction energies of hydrogen bonds with uncoordinated water (ΔE, kcal mol^{-1}) are given

Type	Chg	Composition	OS	CN	OS/CN	Aqua complexes	ESP	d	ΔE	Ammine complexes	ESP	d	ΔE
0	0	Linear Ag(I)	+1	2	0.50	$AgCl(H_2O)$ (**3**)	74.21	1.80	−9.24	$AgCl(NH_3)$ (**79**)	57.60	1.99	−6.02
		Square planar Pd(II)	+2	4		*cis*-$PdCl_2(H_2O)_2$ (**6**)	63.77	1.80	−8.42	*cis*-$PdCl_2(NH_3)_2$ (**82**)	56.00	2.02	−5.44
		Square planar Pt(II)	+2	4		*cis*-$PtCl_2(H_2O)_2$ (**20**)	65.87	1.79	−8.68	*cis*-$PtCl_2(NH_3)_2$ (**96**)	54.75	2.01	−5.63
$1_{0.33}$	1+	Octahedral Co(II)	+2	6	0.33	$CoCl(H_2O)_5^+$ (**41**)	141.07	1.79	−12.72	$CoCl(NH_3)_5^+$ (**119**)	120.67	2.03	−9.02
		Octahedral Ni(II)	+2	6		$NiCl(H_2O)_5^+$ (**47**)	137.80	1.79	−12.53	$NiCl(NH_3)_5^+$ (**125**)	120.48	2.02	−9.28
		Octahedral Zn(II)	+2	6		$ZnCl(H_2O)_5^+$ (**53**)	135.06	1.79	−12.08	$ZnCl(NH_3)_5^+$ (**131**)	122.56	2.02	−9.31
		Octahedral Cd(II)	+2	6		$CdCl(H_2O)_5^+$ (**59**)	128.46	1.81	−11.22	$CdCl(NH_3)_5^+$ (**137**)	119.79	1.99	−8.88
$1_{0.50}$	1+	Linear Ag(I)	+1	2	0.50	$Ag(H_2O)_2^+$ (**4**)	145.85	1.71	−15.01	$Ag(NH_3)_2^+$ (**80**)	128.76	1.90	−10.74
		Square planar Pd(II)	+2	4		$PdCl(H_2O)_3^+$ (**10**)	148.12	1.71	−15.15	$PdCl(NH_3)_3^+$ (**86**)	135.58	1.92	−11.15
		Square planar Pt(II)	+2	4		$PtCl(H_2O)_3^+$ (**24**)	153.06	1.70	−15.48	$PtCl(NH_3)_3^+$ (**100**)	135.89	1.91	−11.36
		Tetrahedral Zn(II)	+2	4		$ZnCl(H_2O)_3^+$ (**34**)	155.02	1.72	−15.26	$ZnCl(NH_3)_3^+$ (**112**)	135.36	1.94	−10.76
		Octahedral Co(III)	+3	6		*cis*-$CoCl_2(H_2O)_4^+$ (**65**)	152.08	1.71	−15.12	*cis*-$CoCl_2(NH_3)_4^+$ (**144**)	132.93	1.96	−12.05
$2_{0.33}$	2+	Octahedral Co(II)	+2	6	0.33	$Co(H_2O)_6^{2+}$ (**43**)	214.39	1.69	−19.58	$Co(NH_3)_6^{2+}$ (**124**)	186.06	1.95	−14.21
		Octahedral Ni(II)	+2	6		$Ni(H_2O)_6^{2+}$ (**49**)	212.83	1.71	−18.89	$Ni(NH_3)_6^{2+}$ (**130**)	194.60	1.96	−14.50
		Octahedral Zn(II)	+2	6		$Zn(H_2O)_6^{2+}$ (**55**)	211.62	1.71	−18.93	$Zn(NH_3)_6^{2+}$ (**136**)	190.67	1.96	−14.02
		Octahedral Cd(II)	+2	6		$Cd(H_2O)_6^{2+}$ (**61**)	196.83	1.71	−18.09	$Cd(NH_3)_6^{2+}$ (**142**)	183.63	1.96	−13.07
$2_{0.50}$	2+	Square planar Pd(II)	+2	4	0.50	$Pd(H_2O)_4^{2+}$ (**15**)	236.33	1.60	−25.34	$Pd(NH_3)_4^{2+}$ (**91**)	210.39	1.82	−17.64
		Square planar Pt(II)	+2	4		$Pt(H_2O)_4^{2+}$ (**29**)	241.20	1.60	−25.41	$Pt(NH_3)_4^{2+}$ (**105**)	212.41	1.81	−17.73
		Tetrahedral Zn(II)	+2	4		$Zn(H_2O)_4^{2+}$ (**37**)	233.69	1.62	−23.97	$Zn(NH_3)_4^{2+}$ (**115**)	202.34	1.84	−16.78
		Octahedral Co(III)	+3	6		$CoCl(H_2O)_5^{2+}$ (**68**)	234.43	1.66	−23.30	$CoCl(NH_3)_5^{2+}$ (**147**)	210.95	1.88	−18.46
3	3+	Octahedral Co(III)	+3	6	0.50	$Co(H_2O)_6^{3+}$ (**73**)	331.01	1.57	−35.15	$Co(NH_3)_6^{3+}$ (**152**)	287.74	1.80	−25.58

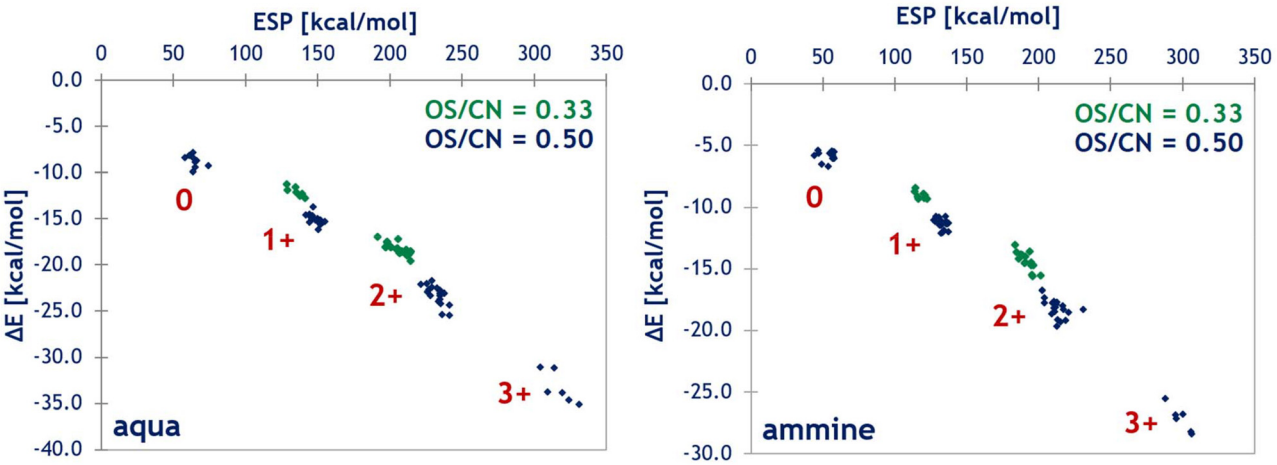

Fig. 2 Electrostatic potential (ESP) *vs.* interaction energy (ΔE) plots for hydrogen bonds of aqua and ammine complexes studied in this work. The red labels indicate the charges of the complexes. OS/CN ratios are indicated accordingly, where OS denotes the metal oxidation state, while CN is the metal coordination number. Interaction energies are calculated at the M06L-D3/def2-TZVPP level of theory.

have an OS/CN value of 0.33 and, among themselves, similar hydrogen bonding energies; however their hydrogen bonds will be weaker (*e.g.* system **53**, −12.08 kcal mol^{-1}) than those of complexes with an OS/CN value of 0.50 (Table 1).

One can anticipate that the OS/CN value is proportional to the part of positive charge that is transferred from the metal to the ligands, namely, an increase of the metal oxidation state increases the hydrogen bonding energy, since the electrostatic potential on interacting hydrogen[43] is more positive (Tables 1, S2 and S3†). For example, we can compare a 1+ charged octahedral Co(II) complex ($[CoCl(H_2O)_5]^+$, **41**, type $1_{0.33}$) and an octahedral Co(III) complex (*cis*-$[CoCl_2(H_2O)_4]^+$, **65**, type $1_{0.50}$) (Table 1). The electrostatic potentials for these Co(II) and Co(III) complexes are 141.07 and 152.08 kcal mol^{-1}, and hydrogen bonding energies are −12.72 and −15.12 kcal mol^{-1}, respectively. A similar trend can be observed for complexes with charge 2+, as well as for ammine complexes (Table 1). On the other hand, the increase in the coordination number causes a decrease of the electrostatic potentials. For example, considering complexes with charge 2+, an octahedral Zn(II) complex ($[Zn(NH_3)_6]^{2+}$, **136**, type $2_{0.33}$) has an ESP on interacting hydrogen of 190.67 kcal mol^{-1} and an interaction energy of −14.02 kcal mol^{-1}, while a tetrahedral Zn(II) complex ($[Zn(NH_3)_4]^{2+}$, **115**, type $2_{0.50}$) has an ESP on interacting hydro-

gen of 202.34 kcal mol^{-1} and an interaction energy of −16.78 kcal mol^{-1} (Table 1).

As shown above, the similar hydrogen bonding energies of complexes with the same OS/CN values are the consequence of similar electrostatic potentials on interacting hydrogen atoms. The Symmetry Adapted Perturbation Theory (SAPT) analysis[44] performed in the PSI4 program (version 1.7.0)[45] of all calculated hydrogen bonds supports the importance of the OS/CN value as a factor influencing the hydrogen bond strength. Namely, SAPT analysis shows that electrostatics is the main component in the interaction energy (Fig. 3 and Tables S2, S3†), encompassing 60–70% and 65–75% of the total attractive interaction for aqua and ammine hydrogen bonds, respectively (Tables S2 and S3†). The electrostatic component follows the trend of the total interaction energy, having different values for complexes with OS/CN values 0.50 and 0.33, with the same charge (Fig. 3 and Tables S2, S3†). Interestingly, within the complexes of the same type all energy components are very similar as well, as indicated by the very small values of standard deviation (Fig. 3). This shows that the nature of hydrogen bonds of all complexes categorized within a certain type is the same. The second most important energy component is induction, representing 20–30% and 15–25% of the total attractive interaction for aqua and ammine hydrogen bonds, respectively (Tables S2 and S3†). For both types of complexes, dispersion does not surpass 15% of the attractive energy components (Tables S2 and S3†).

In addition to complexes with π-donor chloride ligands (Table 1), we also studied hydrogen bonds of complexes containing cyanide (structures **164–182**, Tables S5 and S6†), which is a π-acceptor ligand. The calculated energies of hydrogen bonds are similar, indicating that the influence of the OS/CN ratio on the hydrogen bonds of water and ammonia complexes is independent of the presence of π-donor or π-acceptor ligands in the complex.

Most of the typical metal complexes, like metal complexes presented in Table 1, contain metals in the oxidation state +2 or +3 and coordination numbers six and four. The most common complexes therefore have OS/CN values of 0.50 or 0.33. We have additionally considered several complexes with unusual OS/CN values (Fig. 1 and Table S4†). By considering aqua and ammine complexes of zinc(II) with varying numbers of ligands, we have shown a linear dependence of hydrogen bond energy on the OS/CN value (Fig. 4). If a wider range of OS/CN values is observed by including the aqua and ammine complexes of sodium(I), the relationship between the interaction energy and OS/CN value remains highly linear (Fig. 4). The complexes with unusual OS/CN values further support our observation that hydrogen bond energy depends on the OS/CN values and show that interactions decrease linearly when OS/CN decreases.

As shown in our previous works,[5–11] hydrogen bond energies become stronger with the increase of the charge of the complex. Here we show that the relationship between the charge and the interaction energy is also linear, as long as the OS/CN value remains constant (Fig. 5).

Our observations on the influence of charge and OS/CN values are supported by analyzing previous data on hydrogen bonds of coordinated ethylenediamine[7] and coordinated amino acids.[8,9] The results show that the hydrogen bonds of complexes with OS/CN values of 0.50 have very similar hydrogen bond energies. Also, complexes with OS/CN values of 0.50 form stronger hydrogen bonds than complexes with OS/CN values of 0.33 (Tables S7 and S8†). Interestingly, the same influence of OS/CN values was observed for OH/π and NH/π interactions between aqua and ammine complexes and aromatic rings (Table S9†).[10,11]

In summary, our extensive gas-phase computational work on hydrogen bonds in the second coordination sphere of metal complexes showed the decisive influence of the charge

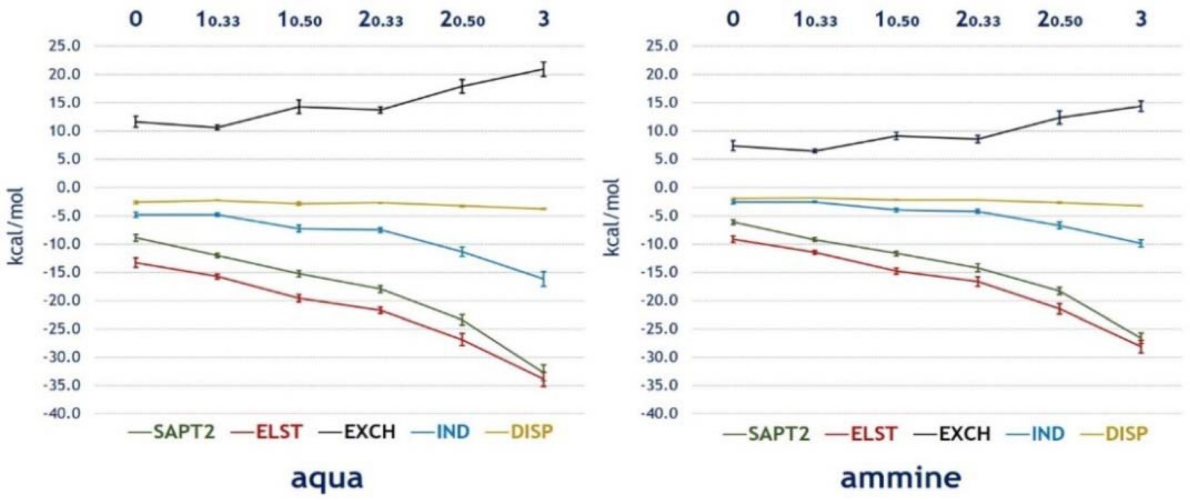

Fig. 3 SAPT2/def2-TZVP interaction energy components for hydrogen bonds of all observed types of complexes, with their standard deviations. The energy components are electrostatic (ELST), exchange (EXCH), induction (IND) and dispersion (DISP).

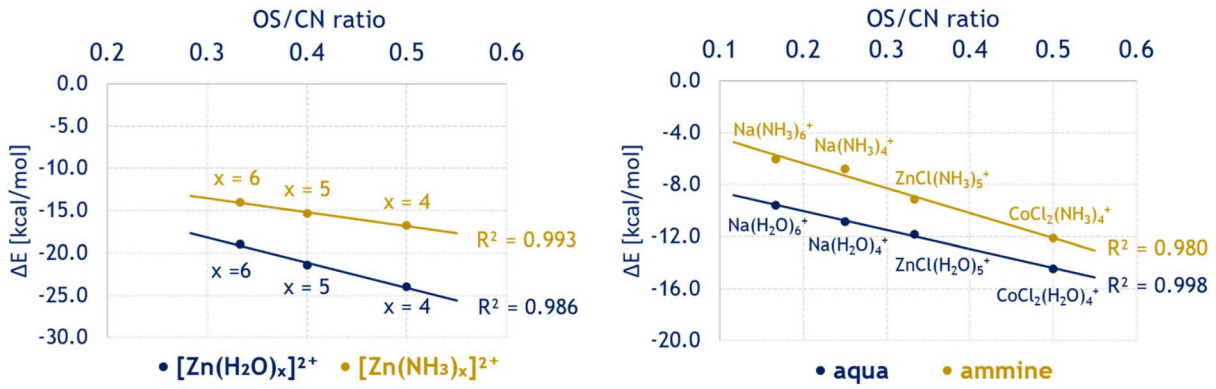

Fig. 4 Correlations between the OS/CN ratios of selected aqua and ammine complexes of the same charge and M06L-D3/def2-TZVPP interaction energies (Δ*E*) of their hydrogen bonds.

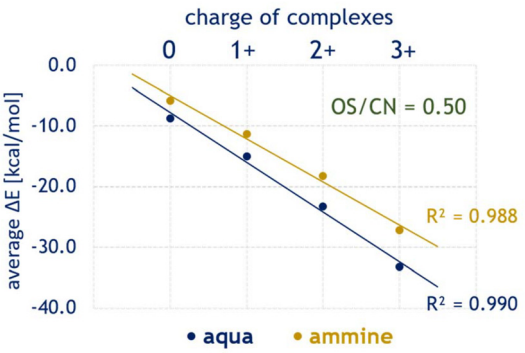

Fig. 5 Correlations between the charge of aqua and ammine complexes with an OS/CN value of 0.50 and average M06L-D3/def2-TZVPP interaction energies of their hydrogen bonds (Tables S2 and S3†).

and ratio of the metal oxidation state and coordination number (OS/CN) on their strength, with all other influences being marginal. Based on our data it is possible to predict and control the strength of hydrogen bonds in various metal complexes. This enables the tuning of hydrogen bonds in the second coordination sphere, with potential applications to other properties in this region of metal complexes, particularly important in the field of catalysis.

Author contributions

The manuscript was written through contributions of all authors. All authors have given approval to the final version of the manuscript.

Conflicts of interest

There are no conflicts to declare.

Data availability

The data supporting this article have been included as part of the ESI.†

Acknowledgements

This work was funded by the Ministry of Science, Technological Development and Innovations of the Republic of Serbia (Agreements No. 451-03-136/2025-03/200288 and 451-03-136/2025-03/200168). The authors would like to thank the IT Research Computing Group at Texas A&M University at Qatar, which is funded by the Qatar Foundation for Education, Science and Community Development, for providing a part of High Performance Computing resources needed for this work. We would also like to acknowledge Dr Marina Andrić from Free University of Bozen-Bolzano, Bolzano, Italy, for her work on the Python script for calculations of electrostatic potentials.

References

1 W. Liu, P. J. Das, H. M. Colquhoun and J. F. Stoddart, *CCS Chem.*, 2022, **4**, 755.
2 D. M. Driscoll, H. Liu, B. Reinhart, I. Popovs, V. Bocharova, S. Jansone-Popova, D. Jiang and A. S. Ivanov, *J. Phys. Chem. Lett.*, 2022, **13**, 12076.
3 L. He, B. Li, Z. Ma, L. Chen, S. Gong, M. Zhang, Y. Bai, Q. Guo, F. Wu, F. Zhao, J. Li, D. Zhang, D. Sheng, X. Dai, L. Chen, J. Shu, Z. Chai and S. Wang, *Sci. China: Chem.*, 2023, **66**, 783.
4 H.-C. Ma, S.-C. Hsiao and Y.-H. Wang, *Catal. Sci. Technol.*, 2023, **13**, 1598.
5 J. M. Andrić, G. V. Janjić, D. B. Ninković and S. D. Zarić, *Phys. Chem. Chem. Phys.*, 2012, **14**, 10896.
6 J. M. Živković, D. Z. Veljkovic and S. D. Zarić, *Cryst. Growth Des.*, 2021, **22**, 148.

7 J. M. Živković, M. R. Milovanović and S. D. Zarić, *Cryst. Growth Des.*, 2022, **22**, 5198.
8 S. S. Zrilić, J. M. Živković and S. D. Zarić, *J. Inorg. Biochem.*, 2023, **242**, 112151.
9 S. S. Zrilić, J. M. Živković and S. D. Zarić, *J. Inorg. Biochem.*, 2024, **251**, 112442.
10 D. Z. Vojislavljević, G. V. Janjić, D. B. Ninković, A. Kapor and S. D. Zarić, *CrystEngComm*, 2013, **15**, 2099.
11 J. P. Blagojević Filipović, D. Z. Vojislavljević-Vasilev and S. D. Zarić, *Cryst. Growth Des.*, 2024, **24**, 1705.
12 T. Ishizuka, T. Kogawa, C. Ogawa, H. Kotani, Y. Shiota, K. Yoshizawa and T. Kojima, *JACS Au*, 2023, **3**, 2813.
13 N. G. Boekell and R. A. Flowers, *Chem. Rev.*, 2022, **122**, 13447.
14 C. M. Galvin, D. P. Marron, J. M. Dressel and R. M. Waymouth, *Complex Inorg. Chem.*, 2023, **63**, 2954.
15 A. B. Emily and J. C. Peters, *J. Am. Chem. Soc.*, 2022, **144**, 21337.
16 S. Sinhababu, R. P. Singh, M. R. Radzhabov, J. Kumawat, D. H. Ess and N. P. Mankad, *Nat. Commun.*, 2024, **15**, 1315.
17 N. G. Boekell, C. O. Bartulovich, S. Maity and R. A. Flowers, *Inorg. Chem.*, 2023, **62**, 5040.
18 R. Flowers and N. O. Ugochinyere, *Dalton Trans.*, 2024, **53**, 2413.
19 C. T. Supuran, *Bioorg. Med. Chem. Lett.*, 2023, 129411.
20 M. Zhao, H. B. Wang, L. N. Ji and Z. W. Mao, *Chem. Soc. Rev.*, 2013, **42**, 8360.
21 R. Essmann, *J. Mol. Struct.*, 1995, **356**, 201.
22 R. Eβmann and C. Mockenhaupt, *Spectrochim. Acta, Part A*, 1996, **52**, 1897.
23 P. J. Farmer, J. R. Cave, T. M. Fletcher, J. A. Rhubottom Jr and J. A. Walmsley, *Inorg. Chem.*, 1991, **30**, 3414.
24 J. N. Reek, B. de Bruin, S. Pullen, T. J. Mooibroek, A. M. Kluwer and X. Caumes, *Chem. Rev.*, 2022, **122**, 12308.
25 S. Ahmad and M. Bühl, *ChemCatChem*, 2024, e202401053.
26 J. F. K. Kotyk, C. M. Hanna, R. L. Combs, J. W. Ziller and J. Y. Yang, *Chem. Sci.*, 2018, **9**, 2750.
27 T. Wititsuwannakul, T. Mukherjee, M. B. Hall and J. A. Gladysz, *Organometallics*, 2020, **39**, 81149.
28 A. Fanourakis, P. J. Docherty, P. Chuentragool and R. J. Phipps, *ACS Catal.*, 2020, **10**, 10672.
29 J. Trouvé and R. Gramage-Doria, *Chem. Soc. Rev.*, 2021, **50**, 3565.
30 J. Y. Li, P. P. Xie, T. Zhou, P. F. Qian, Y. B. Zhou, H. C. Li, X. Hong and B. F. Shi, *ACS Catal.*, 2022, **12**, 9083.
31 A. Franchino, Á. Martí and A. M. Echavarren, *J. Am. Chem. Soc.*, 2022, **144**, 3497.
32 À. Martí, G. Ogalla and A. M. Echavarren, *ACS Catal.*, 2023, **13**, 10217.
33 P. Elías-Rodríguez, M. Benítez, J. Iglesias-Sigüenza, E. Díez, R. Fernández, J. M. Lassaletta and D. Monge, *Org. Lett.*, 2024, **26**, 5995.
34 À. Martí, M. Montesinos-Magraner, A. M. Echavarren and A. Franchino, *Eur. J. Org. Chem.*, 2022, e202200518.
35 B. Deborah, J. A. Bogart, D. L. Ross, J. W. Ziller and A. S. Borovik, *Inorg. Chim. Acta*, 2019, **495**, 118960.
36 T. Kitanosono, T. Hisada, Y. Yamashita and S. Kobayashi, *Angew. Chem.*, 2021, **133**, 3449.
37 M. J. Frisch, G. W. Trucks, H. B. Schlegel, G. E. Scuseria, M. A. Robb, J. R. Cheeseman, G. Scalmani, V. Barone, G. A. Petersson, H. Nakatsuji, X. Li, M. Caricato, A. Marenich, J. Bloino, B. G. Janesko, R. Gomperts, B. Mennucci, H. P. Hratchian, J. V. Ortiz, A. F. Izmaylov, J. L. Sonnenberg, D. Williams-Young, F. Ding, F. Lipparini, F. Egidi, J. Goings, B. Peng, A. Petrone, T. Henderson, D. Ranasinghe, V. G. Zakrzewski, J. Gao, N. Rega, G. Zheng, W. Liang, M. Hada, M. Ehara, K. Toyota, R. Fukuda, J. Hasegawa, M. Ishida, T. Nakajima, Y. Honda, O. Kitao, H. Nakai, T. Vreven, K. Throssell, J. A. Montgomery Jr., J. E. Peralta, F. Ogliaro, M. Bearpark, J. J. Heyd, E. Brothers, K. N. Kudin, V. N. Staroverov, T. Keith, R. Kobayashi, J. Normand, K. Raghavachari, A. Rendell, J. C. Burant, S. S. Iyengar, J. Tomasi, M. Cossi, J. M. Millam, M. Klene, C. Adamo, R. Cammi, J. W. Ochterski, R. L. Martin, K. Morokuma, O. Farkas, J. B. Foresman and D. J. Fox, *Gaussian 09, Revision D.01*, 2016.
38 Y. Zhao and D. G. Truhlar, *Theor. Chem. Acc.*, 2008, **120**, 215.
39 S. Grimme, J. Antony, S. Ehrlich and H. A. Krieg, *J. Chem. Phys.*, 2010, **132**, 154104.
40 F. Weigend and R. Ahlrichs, *Phys. Chem. Chem. Phys.*, 2005, **7**, 3297.
41 J. S. Murray and P. Politzer, *Wiley Interdiscip. Rev.: Comput. Mol. Sci.*, 2017, **7**, e1326.
42 J. M. Andrić, M. Z. Misini-Ignjatović, J. S. Murray, P. Politzer and S. D. Zarić, *ChemPhysChem*, 2016, **17**, 2035.
43 ESP were calculated on interacting hydrogen atoms at the 0.001 a.u. electron density contour, using inhouse Python script for ESP calculations. This script relies on Gaussian cube files with electron density and ESP data, and it can be accessed *via* the following link: **https://github.com/JelenaZi/ESP-Calculator/**. This link also contains instructions, examples of Gaussian cube files, input and output files.
44 B. Jeziorski, R. Moszynski and K. Szalewicz, *Chem. Rev.*, 1994, **94**, 1887.
45 R. M. Parrish, L. A. Burns, D. G. A. Smith, A. C. Simmonett, A. E. DePrince, E. G. Hohenstein, U. Bozkaya, A. Yu. Sokolov, R. Di Remigio, R. M. Richard, J. F. Gonthier, A. M. James, H. R. McAlexander, A. Kumar, M. Saitow, X. Wang, B. P. Pritchard, P. Verma, H. F. Schaefer, K. Patkowski, R. A. King, E. F. Valeev, F. A. Evangelista, J. M. Turney, T. D. Crawford and C. D. Sherrill, *J. Chem. Theory Comput.*, 2017, **13**, 3185.